Enhancing Biofidelity of THUMS 50th Percentile Male Foot and Ankle: Refinements and Validations.

Ramakrishnan Balaji Iyer, Bronislaw Gepner, Jason Hallman, Koji Onishi, Yoshiharu Sonoda, Jason L. Forman

Abstract Accurately predicting ankle injuries in motor vehicle collisions (MVCs) using human body model (HBM) simulations requires appropriate anatomic precision and biofidelity in an ankle joint model. The study aims to refine the foot and ankle joints of the Total Human Model for Safety (THUMS) v.6.1 50th percentile male (AM50) occupant model and assess the biofidelity of the model against available Post-Mortem Human Subjects (PMHS) data. Refinement included the addition of select ligaments and morphing and adjustment of existing model's ankle ligament and their insertion points to enhance anatomical accuracy. Additionally, the constitutive material model of all the ankle ligaments was changed. Cartilage also was added on the articulating surfaces of ankle bones to improve continuity of load transfer. This updated model was validated by performing four biofidelity cases - compressive axial impact, dorsiflexion, inversion, and eversion - replicating experiments conducted on male PMHS. The model showed good agreement for all cases compared to PMHS data. Finally, a standard male Mil-Spec shoe model was fitted to the THUMS AM50 foot by a reproducible process. The refinement carried to the ankle joint has improved the anatomical representation and the biofidelity. The addition of the shoe is also a significant improvement, allowing for more representative simulation of ankle loading in likely real-world scenarios.

Keywords Ankle biofidelity evaluation, 50th percentile male, THUMS, Finite Element Human Body Model, Shoe fitting.

I. INTRODUCTION

Ankle injuries are among the most frequently observed AIS2+ injuries in belted occupants involved in frontal impact motor vehicle collisions (MVCs) [1–2]. Understanding the mechanism of ankle fractures allows for developing effective counter measures to prevent such injuries. But, due to the complex structure of the ankle joint and the variety of loading conditions it experiences during the MVCs, predicting ankle injury risk remains a significant challenge. Human body models (HBMs) offer a powerful computational tool for injury prediction research, with the potential to assess bone failure and tissue/ligament-level responses under different loading scenarios. As HBMs continue to evolve, they may complement traditional physical safety assessments in the future. For HBMs to accurately predict injury risk, they must exhibit both anatomical accuracy, precision and biofidelity. Validation of HBMs ensures their responses reliably represent human biomechanics. These validations are conducted at multiple levels, including local bones, joints, and full-body assessments, often against PMHS test data.

THUMS is one such HBM that has been developed with a high degree of anatomical detail and has been validated across multiple body regions, including the head, neck, chest, abdomen, pelvis, and extremities. The current THUMS v6.1 AM50 lower extremity validation suite includes validation through knee-thigh-hip (KTH) impact tests and three-point bending tests of the femur and tibia. However, for the ankle joint, validation is limited to axial foot impact tests, both with and without a constant Achilles tendon force. Given the complex ways in which the ankle can be loaded and injured in MVCs, it is helpful to refine and evaluate the biofidelity of the HBM ankle under various loading conditions.

The THUMS v.6.1 AM50 ankle joint primarily consists of the distal ends of the tibia and fibula, along with the talus and calcaneus bones, interconnected by various ligaments. In the baseline model, the ligaments connecting the tibia-fiblua, tibia-talus, fibula-talus and fibula-calcaneus were attached to elements or nodes forming the

R. B. Iyer (+1-434-257-3722, zdf5ks@virginia.edu) is a Research Engineer, B. Gepner is a Senior Scientist and J. Forman is an Associate Professor at Centre for Applied Biomechanics at University of Virginia, USA. K. Onishi is an Assistant Manager and Y. Sonoda is a Research Engineer at Toyota Motor Corporation. J. Hallman is a Senior Research Manager at Collaborative Safety Research Center, Toyota Motor North America R&D.

articulating surfaces (corner elements and nodes of the bone), whereas anatomically ankle ligaments were observed approximately 5mm away from these surfaces [3–4]. This misalignment may affect the model's ability to replicate realistic ligament behavior under loading conditions. Such observations were highlighted in past biofidelity simulations with the THUMS American 5th percentile female (THUMS AF05) HBM with similar ligament geometries and material models [5]. In particular biofidelity simulations, one ligament exhibited forces exceeding reported failure tolerance while the remaining ligaments experienced substantially lower forces. This observation suggests what was likely unrealistic load-sharing dynamics. The baseline model was also missing the plantar ligament which contributes to foot stability and enhances biofidelity.

In the original model gaps of approximately 6mm were observed between the distal tibia and talus, as well as between the talus and calcaneus bones. These voids could impact joint stability and load transfer. Similar gaps had been observed previously in other HBMs and have been addressed by adding layers of cartilage over the articulating surfaces of the bones (also providing for a more realistic contact stiffness [5–6]. Finally, the baseline THUMS AM50 model does not have any footwear. Although footwear does not necessarily change the injury tolerance, it can affect the foot interaction with the pedals and footwell thereby influencing the ankle kinematics and loading [6]. Given that physical crash tests are routinely conducted with shoes and also that vehicle occupants generally wear shoes, incorporating a shoe model into the Human Body Model (HBM) would enhance the applicability of simulations to tests and field data. This addition could more accurately capture ankle loading patterns and injury mechanisms observed in automotive crash scenarios.

This study focuses on refinement and enhancement of the foot and ankle joint in THUMS v.6.1 AM50 to improve the biofidelity of the ankle joint and anatomical accuracy. The enhancement began with improving the anatomical representation of the ankle ligaments followed by the addition of cartilage. The updated model with updated ligaments and cartilage was evaluated against testing conducted on 50th percentile male PMHS without shoes under four ankle loading scenarios: compressive axial impact, dorsiflexion, inversion, and eversion. Finally, a finite element (FE) shoe was integrated through a reproducible fitting process resulting in a snug fit, and the updated foot and ankle with shoes was re-integrated into the whole HBM.

II. METHODS

Ankle Ligaments Refinements

The refinements were carried out on the existing THUMS AM50 v.6.1 by improving the anatomic accuracy (referring to the enhancement of ligament insertion points by aligning them more closely with documented anatomical landmarks) of the ankle ligaments and updating their material model.

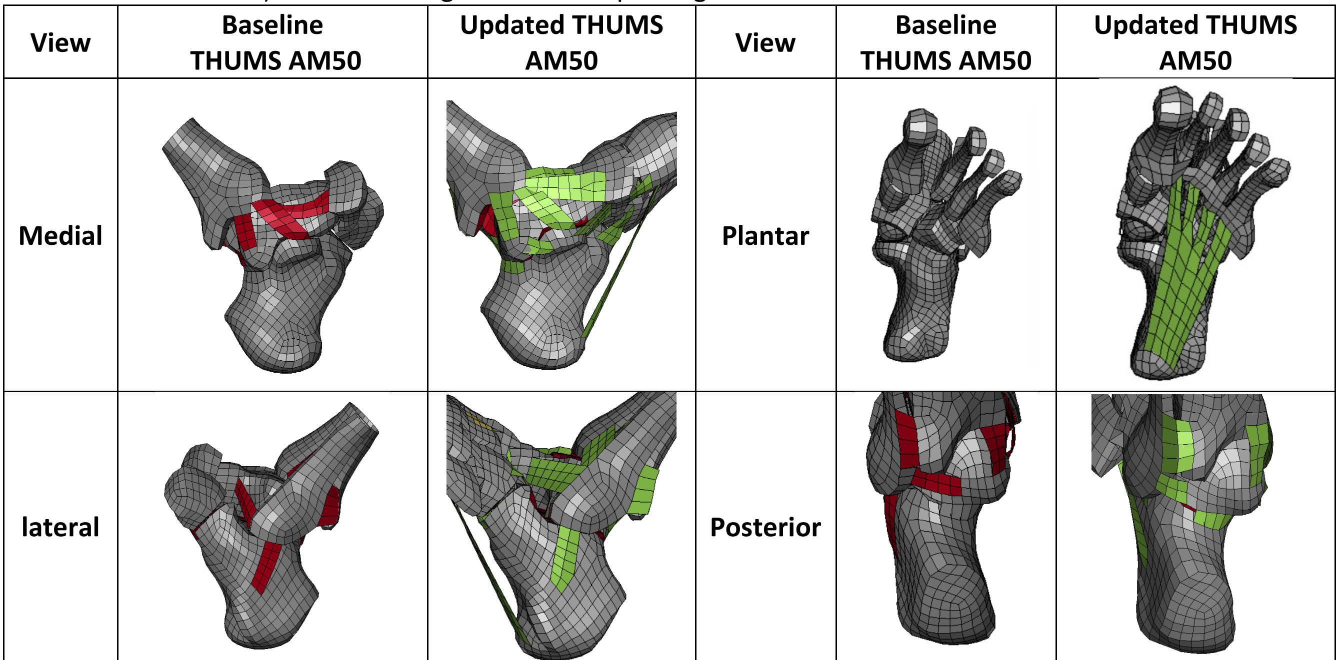

Fig. 1. Illustration of morphed ankle ligaments (green color) in THUMS AM50 shown in different view compared to the baseline model (red color).

The refinements were implemented based on several anatomic references [7–10], which led to the incorporation of certain previously omitted ligaments and adjustment of ligament insertion points to consider the movements of the ankle joint with respect to articulating surfaces.

After an initial trial at improving the anatomic accuracy of the existing ankle ligaments, their placement was further refined by applying local morphing, element-node aligning, and node translations to improve the mesh quality and remove the slack from the ligaments. Select omitted ligaments such as the plantar ligament were incorporated, and the insertion points were adjusted by attaching the ligaments to nodes at 5–7mm from the articulating surface. Figure 1 shows the updated THUMS AM50 model with refined ankle ligaments. A surface-to-surface contact interaction was defined between each specific ankle ligament and the neighboring bones to accurately capture their mechanical interface. Additionally, it was previously observed that the force-displacement behavior of ankle ligaments during the PMHS testing generally exhibited a hyperelastic response [5]. Therefore, in that study, the ankle ligaments' material model was changed from fabric to hyperelastic material model: **MAT_OGDEN_RUBBER*. The updated material model led to more even distribution in the load shared across the ligaments instead of the dominance in the force by a singular ligament which was observed during the usage of **MAT_Fabric*. So, the same material model was adapted to the current THUMS AM50 ankle ligament refinement process.

Modeling Ankle Cartilage

After the ankle ligament refinement, the next enhancement consisted of adding cartilage to the model. To enhance contact mechanics and load distribution between ankle bones, cartilage was incorporated at the distal ends of the tibia and fibula, as well as on the talus and calcaneus. The modeling approach outlined in the study [5] was adopted to model cartilage. Special consideration was given to adjust the cartilage thickness to effectively bridge the gaps between these bones. Based on insights from previous studies [5], the cartilage thickness was defined within a range of 1 mm to 4 mm.

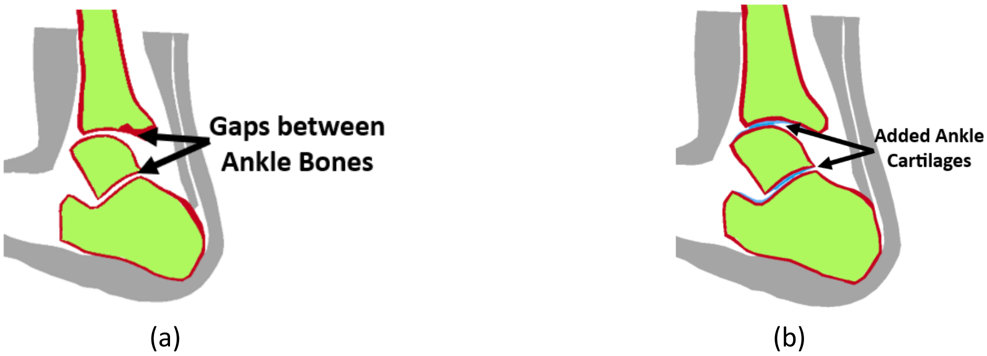

Fig. 2. Cross section of the THUMS AM50 ankle (a) before (b) after addition of the cartilage added to the various articular surfaces of the ankle (highlighted in red color).

(a) Tibia Talus Cartilage (b) Tibia Calcaneus Cartilage (c) Ankle Cartilage

Fig. 3 Illustration of anterior view of ankle joint highlighting the cartilage (blue – Inferior and superior talus cartilages and red color – other cartilages) added to the various articular surfaces of the ankle

The mid-substance of the cartilage was primarily modeled using hexahedral elements to ensure stability and accurate mechanical behavior as the adjacent elements consist of similar element type. To ensure a seamless transition between cartilage and bone, the peripheral cartilage elements were modified into tetrahedral or pentahedral elements. An illustration of the THUMS AM50 model before and after cartilage integration is presented in Fig. 2, while Fig. 3 provides a detailed view of the ankle bone with the newly incorporated cartilage.

Given the significantly lower stiffness of cartilage compared to bone, it was assigned a **MAT_ELASTIC* material model with a density of 2.0E-06 kg/mm³ and a Young's modulus of 200 MPa [5]. To facilitate efficient load transfer across cartilage surfaces, **AUTOMATIC_SURFACE_TO_SURFACE* a contact definition was implemented.

Validation of THUMS AM50 Ankle (Barefoot)

To evaluate the biofidelity of the refined and enhanced THUMS AM50 foot and ankle (barefoot), validation cases of compressive axial impact, dorsiflexion, inversion, and eversion were performed based on past experiments conducted on male PMHS which are summarised in Table 1. These validation cases were repeated for the baseline THUMS AM50 model and compared against the updated THUMS AM50.

Table 1 Summary of Validation Cases

Validation Case	Reference	Number of PMHS
Axial Impact	Funk *et al*., (1999) [11]	10
Dorsiflexion	Rudd *et al*., (2004) [12]	12
Inversion & Eversion	Funk *et al.* (2002) [13]	6 (Inversion) & 5 (Eversion)

Axial Impact

Reference [11] conducted dynamic axial impact on 10 cadaver legs. The leg was placed horizontally in the test rig and the knee was constrained in an adjustable knee block. The ankle was positioned in a neutral orientation for every test. One or two layers of 3/8" (9.5 mm) foam padding were placed between the foot and the footplate, and 1" (25.4 mm) foam padding was placed around the knee for load distribution. The femur was tied back to prevent flexion of the knee during impact. The knee block position was adjusted to compress the instrumented leg until it was axially preloaded to half of the specimen's body weight immediately prior to impact. A high level of impact energy (~ 800 J) was used for all testing. The effective mass of the pendulum was 33 kg, and the impact velocity was 7 m/s. A section of the tibia was removed to accommodate a five-axis load cell while preserving the original orientation of the bone ends in all six degrees of freedom.
These tests conditions were reconstructed in simulation. First, the left lower extremity was separated from the mid shaft femur from the updated THUMS AM50 and the knee was flexed at a 90° angle as in the PMHS test as shown in Fig. 4 (a). Next, a knee foam padding representing an idealized case was modeled by extracting the THUMS AM50 knee skin surface elements and offsetting it by 25mm normal to the elements. The outer surface of the knee pad was constrained in all degrees of freedom (DOF). **AUTOMATIC_SURFACE_TO_SURFACE* contact was defined between the knee skin and the knee form pad. Also, a rigid plate was modelled and positioned on the planter surface of the foot representing the impactor. This rigid plate impactor face was driven via prescribed motion and the displacement time history was based on the average impactor motion time history measured during the tests. The setup of the axial impact simulation is shown in Fig. 4 (a).

Dorsiflexion

Reference [12] performed 12 male PMHS tests to investigate the ankle dorsiflexion response and injury response of the foot and ankle by loading a brake pedal into the forefoot. A test fixture was constructed such that a simplified, yet realistic, pedal load was applied to the forefoot, forcing the foot into dorsiflexion. Leg specimens were placed in the test apparatus with the knee constrained in an adjustable block (Fig. 4 (b)). Foam padding was placed around the knee, and the femur was tied back to prevent flexion of the knee during impact. A strap was placed around the proximal end of the tibia, just distal to the knee joint, to support the leg vertically similar to that of axial impact. PMHS specimens were instrumented to measure leg forces and moments, leg/foot accelerations and angular rates, and Achilles tension. Load cell and accelerometer data were used to calculate moments at the ankle joint.
To recreate this testing in simulation, the same lower extremity posture and idealized padding developed for the dynamic axial impact was used here. Instead of a rigid full-foot impactor, a smaller impactor face representing a brake pedal was used to apply force to the forefoot to force the ankle into dorsiflexion. Figure 4 (b) shows the simulation setup for the dorsiflexion validation case.

Inversion and Eversion

Reference [13] conducted tests to study ankle model response in dynamic inversion and eversion. The study was conducted with 11 male PMHS test for inversion (six tests) and eversion (five tests). The experimental setup consisted of a fixture developed to apply dynamic moments about a prescribed ankle center rotation axis. In these tests, the proximal tibia was supported within a rigid potting device. First, a 2 kN axial preload was applied to pre-compress the ankle, followed by the application of approximately 1000°/s rotational velocity about the foot's inversion-eversion axis, centered at the subtalar joint.

These tests were recreated in simulation by constraining the motion of the proximal tibia, applying a static 2 kN axial preload to the leg using the top plate (coupled to the proximal nodes of the tibia plateau using constraint rigid body) shown in Fig .4 (c), and then applying rotation to the calcaneus (coupled to the lower plate via constraint rigid body)via prescribed motion (based on the average calcaneus rotation time history measured in the tests (Fig .4 (c)).

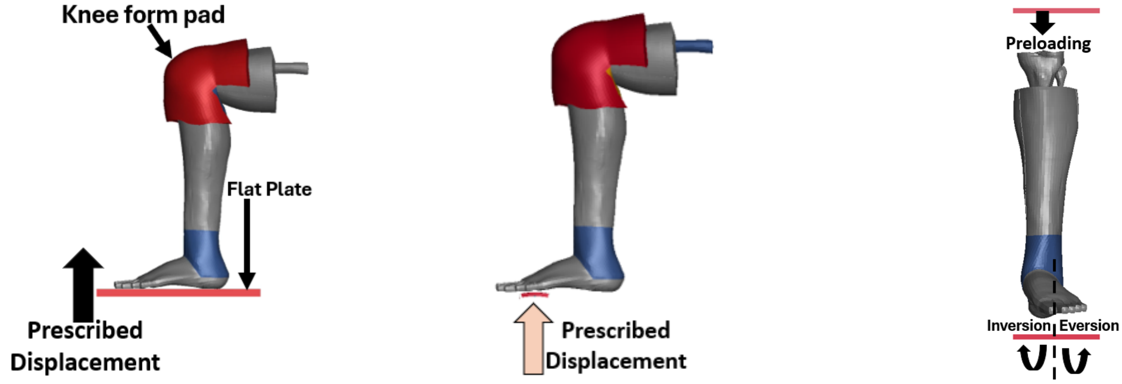

Fig. 4. Illustration of the simulation setup of (a) axial impact (b) dorsiflexion (c) inversion and eversion, targeting the experiments of [7–8] and [9] respectively.

Instrumentation

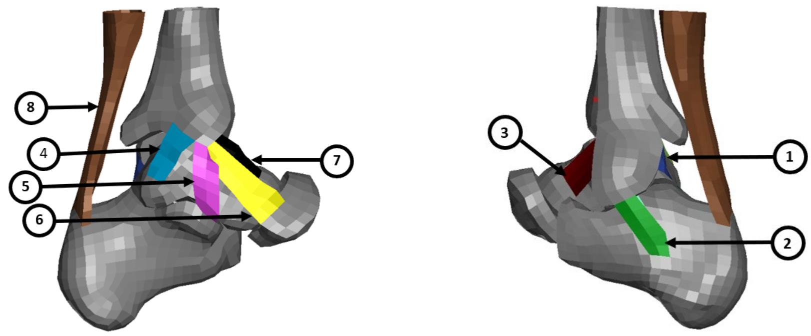

Nr.	Ligament Name
1	TALOFIBULARE_POSTERUS
2	Calcanofibulare
3	TALOFIBULARE_ANTERIOR
4	TALOTIBIULARE_POST
5	TALOTIBULARE_MED_1
6	TALOTIBULARE_MED_2
7	TALOTIBULARE_ANT
8	ACHILLES_TENDON

(e)

Fig. 5. Model instrumentation (a) cross-section force at mid-tibia (b) the moment at the ankle joint centre calculated via transformation of the forces and moments measured in the distal tibia and fibula. Updated THUMS AM50 v6.1 Ankle ligaments (c) lateral (d) medial (e) nomenclature of the ligaments.

Outputs such as the forces and moments were recorded during the simulations to compare against the experimental results. The output forces and moments were measured by defining cross-section areas at the mid and distal tibia (Fig. 5. (a)). The resultant moment at ankle center was computed by performing rigid body moment transformation of the forces and moments measured at the distal tibia (Fig. 5.(b)). Also, the ligament cross-section was defined at their longitudinal center, and the forces were recorded to access the load distribution between the updated ligaments.

Shoe fitting for THUMS AM50

To ensure realistic ankle loading and interaction with the surrounding/vehicle environment and to predict accurate ankle kinematics and injury assessment, it is important to integrate a shoe for use with human body models for crash simulations.

Therefore, a shoe was fitted to the THUMS AM50. The geometry and FE model of this shoe was generated based on a 3D scan of a shoe of a Hybrid III 50th percentile male dummy. The 50th percentile male Hybrid III dummy uses a specific shoe for testing, designed to meet military specification MIL-S-13192P. The shoe fitting methodology previously developed for THUMS AF05 was adapted for use with the THUMS AM50 model [5]. However, preliminary fitting trials revealed considerable gaps between the foot and the inner surface of the shoe, primarily due to the foot's posture—an issue also encountered during the AF05 shoe fitting process. To address this, a pre-simulation step was introduced, in which a flat plate was pressed against the foot to flatten the arch (Fig. 6).

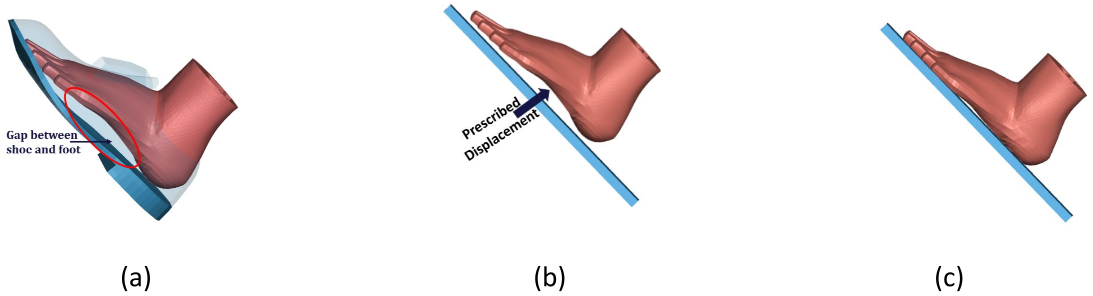

Fig. 6. (a) Preliminary shoe fitting, keeping the initial posture of the foot static, (b) Simulation setup for flattening the foot and, (c) Flattened foot by pressing the flat plate.

Once the arch was adjusted, the shoe fitting process proceeded through the following stages: (i) scaling down the foot, (ii) expanding the foot and ankle within the shoe, (iii) thermally contracting the shoe around the foot, (iv) folding the lace flaps, (v) tightening the laces, and (vi) integrating the foot model with the fitted shoe into the complete body model (Fig. 7). In stages (i) and (ii), the shoe model was initially aligned with the THUMS AM50 foot without any contact and then uniformly scaled up to 1.5 times its original size. In stage (iii) a thermal contraction simulation was performed to eliminate gaps between the shoe and the foot while maintaining continuous contact.

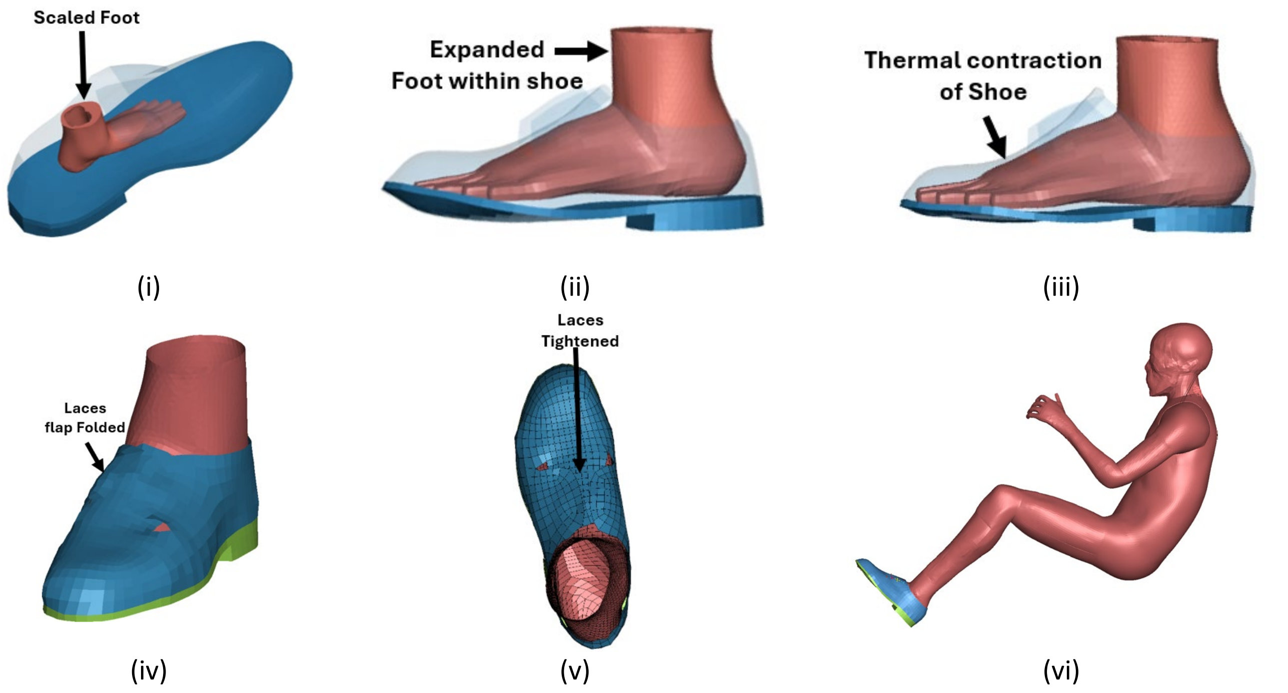

Fig. 7. Shoe fitting process: (i) scaling; (ii) expansion of foot and ankle within the shoe; (iii) thermal contraction of the shoe around the foot; (iv) folding of lace flaps; (v) tightening of laces; (vi) integration of foot model with the fitted shoe into the THUMS.

During this process, the foot was temporarily treated as a rigid body, allowing the shoe to conform precisely to its shape. Subsequently, the lace flaps were folded, and shoelaces—modeled using seatbelt elements—were tightened to achieve a snug, and anatomically realistic fit around the foot. To minimise slipping, the coefficient of friction between the shoe and foot was set to 0.5. Additionally, the upper portion of the shoe was assigned to a thickness of 3.5 mm, based on physical measurements. The combination of a snug fit, lace tensioning, and enhanced friction ensured effective coupling between the THUMS AM50 foot and the shoe.

III. RESULTS

The ankle biofidelity validation simulations for updated THUMS AM50 without shoe were assessed against matched PMHS biofidelity results from cadaver tests conducted without footwear. The same simulation suit was performed for the baseline model and the results were compared against the updated model.

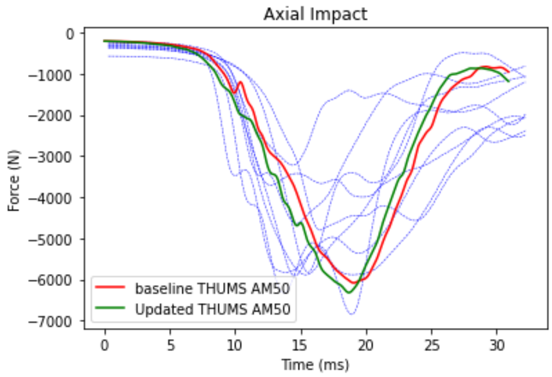

Fig. 8. Axial Impact validation results: Cross-sectional tibia force from the updated THUMS AM50 axial impact simulation (green), compared to the PMHS results [11] and the baseline THUMS AM50 (red).

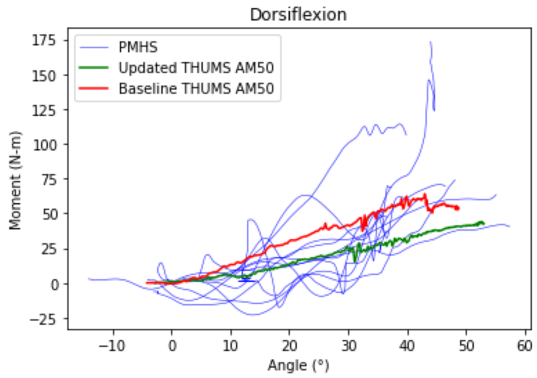

(a) Ankle Moment vs. Angle

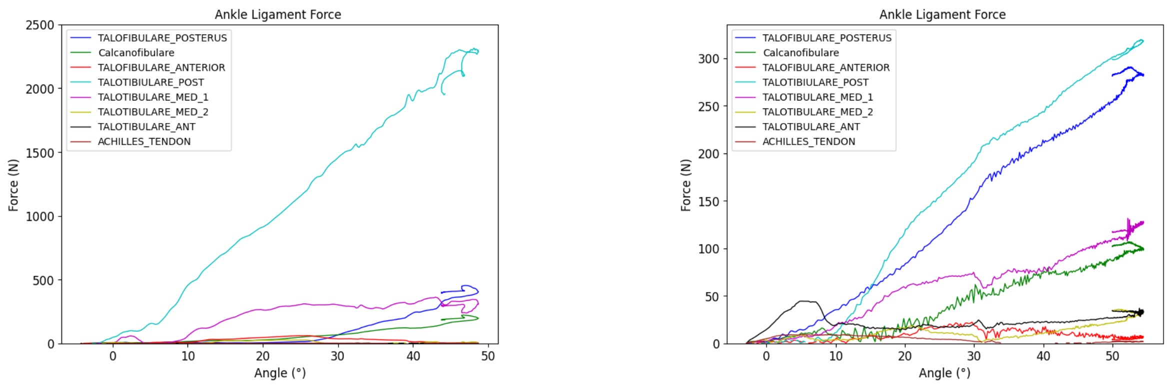

(b) Baseline THUMS AM50 (c) Updated THUMS AM50

Fig. 9. (a) Transformed ankle moment from the updated THUMS AM50 dorsiflexion simulation (green line) vs. the PMHS corridor (blue lines, with the PMHS test results [12]) and baseline THUMS AM50 (red), (b) and (c) cross-section ankle ligament force time history (Note: The Y-axis limits of plot (b) and (c) are different).

For the axial impact validation, the lower extremity (isolated from the model and sectioned from mid-thigh) was positioned on impactor with minimal initial clearance to prevent numerical instability. As described earlier, mid-tibia, cross-section force time history was recorded, and the force-displacement response was compared against the PMHS results (Fig. 8). The model exhibited a peak force of 6130 N. The response closely followed the PMHS results, and the peak force was in-phase with one of the PMHS tests. The peak force of the baseline model resulted slightly less than the result obtained from the updated model (~ 6000N)

For the dorsiflexion validation, a rigid cylindrical impactor was used, and the resulting moment at the ankle centre was recorded and analysed against changes in calcaneus angle. The moment was derived through a rigid body transformation of the force and moment at the distal tibia. The foot angle was determined by tracking the relative rotation between the mid tibia and rotation of calcaneus.

The moment versus calcaneus angle comparison (Fig. 9 (a)) showed close agreement with PMHS data. At 35° of calcaneus rotation, the updated model generated an ankle moment of 23 Nm while the baseline model generated 48 Nm. Figure 9 (b) and Figure 9 (c) show the plot for ligament cross-section forces vs. calcaneus rotation for the updated and the baseline model. For the baseline model, the posterior tibiotalar ligament exhibited 2250 N of cross-section force while the same ligament in the updated model exhibited 325 N. The peak cumulative ligament cross-section forces during dorsiflexion were 3442.5 N for the baseline model and 961 N for the updated model.

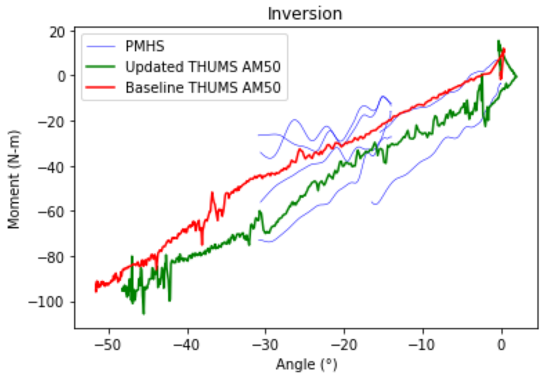

(a) Ankle Moment vs. Angle

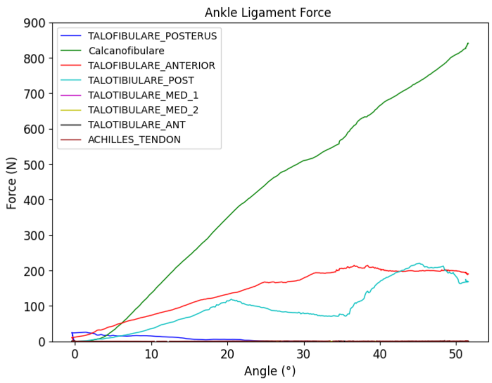

(b) Baseline THUMS AM50

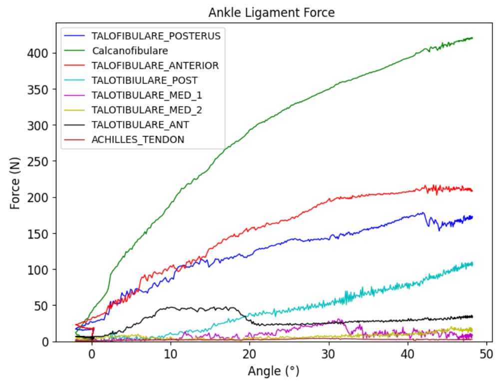

(c) Updated THUMS AM50

Fig. 10. (a) Transformed ankle moment from the updated THUMS AM50 inversion simulation (green line) vs. the PMHS corridor (blue lines, with the PMHS test results [13]) and baseline THUMS AM50 (red), (b) and c) cross-section ankle ligament force time history (Note: The Y-axis limits of plot (b) and (c) are different).

For the inversion and eversion validation cases, the relationship between ankle moment and calcaneus rotation was analyzed and compared with PMHS experimental data. Figure 10 and Figure 11 present the simulation results for inversion and eversion loading scenarios respectively. The ankle moment was computed through a rigid body transformation of the distal tibia moments, following the same methodology used in the dorsiflexion validation. The calcaneus rotation angle was measured relative to the tibia, ensuring consistency with experimental measurements. In the inversion case, the baseline and updated THUMS AM50 models were within the PMHS test ranges, although the updated model exhibited a more compliant response, aligning with the lower boundary of the PMHS corridor. The peak moment reached 95 Nm at a calcaneus rotation of 48° (Fig. 10 (a)). The ligament cross-section forces plotted against the calcaneus rotation are shown in Fig. 10 (b) and Fig. 10 (c) for the updated and the baseline model respectively. The peak cumulative ligament cross-section forces during inversion were 1307.5 N for the baseline model and 1030 N for the updated model. Under eversion loading, the peak values were reaching 6365 N in the baseline model and 1895.1 N in the updated model. The recorded forces for calcaneofibular are 900 N and 400 N for baseline and updated model respectively and is maximum amongst the other ligaments.

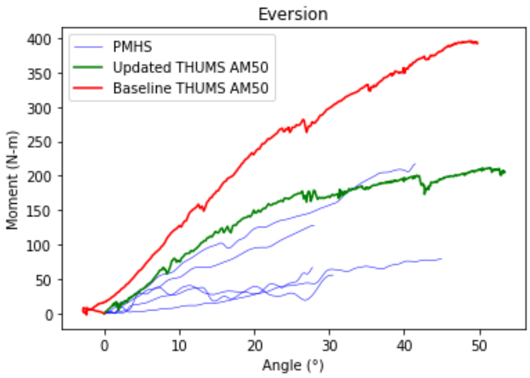

(a) Ankle Moment vs. Angle

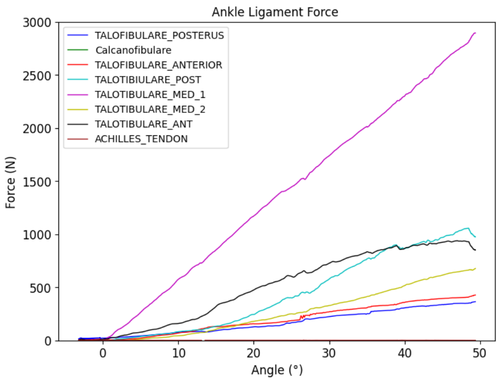

(b) Baseline THUMS AM50

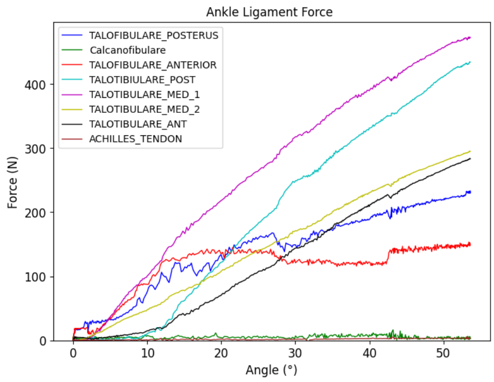

(c) Updated THUMS AM50

Fig. 11. (a) Transformed ankle moment from the updated THUMS AM50 eversion simulation (green line) vs. the PMHS corridor (blue lines, with the PMHS test results) and baseline THUMS AM50 (red), (b) and (c) cross-section ankle ligament force time history (Note: The Y-axis limits of plot (b) and (c) are different).

In the case of eversion, the ankle moment vs. calcaneus rotation is shown in Fig. 11 (a) and the peak moment reached 182 Nm at a calcaneus rotation of 42°. Compared with the baseline model, the updated model response was more compliant and better agreed with the PMHS data. Fig. 11 (b) and Fig. 11 (c) show the plots for cross-section forces of baseline and updated models in eversion, respectively. The talotibular ligament contributed the maximum forces in both the models (2920 N and 494 N for the updated and the baseline model respectively).

IV. DISCUSSION

Ankle injuries are among the most prevalent and complex injuries sustained in motor vehicle collisions (MVCs). Accurate prediction of these injuries is needed to understand underlying mechanisms and identify effective injury mitigation countermeasures. Computational HBMs have been used for injury prediction and prevention research; however, achieving anatomical and biomechanical fidelity is essential for reliable injury assessment in the future.

This study aimed to enhance the anatomical accuracy of the foot and ankle region in the THUMS AM50 model through geometrical refinement and material updates. The plantar ligament that was absent in the baseline model was incorporated, and manual morphing techniques, such element node alignment and node translation, were employed to adjust the existing ankle ligaments and their insertion points to achieve anatomically realistic positioning. The constitutive material model for all ligaments was updated from fabric to an Ogden rubber formulation to better represent their mechanical behavior. Furthermore, cartilage was introduced at the articulating surfaces of the ankle bones to improve joint congruity and ensure continuous load transmission. To validate the updated model, four biofidelity assessment simulations—compressive axial impact, dorsiflexion, inversion, and eversion—were conducted, replicating experimental studies performed on PMHS. The validation metrics included compressive tibial forces and ankle moments relative to calcaneus rotation. Additionally, a standard Mil-Spec shoe model was fitted to the THUMS AM50 foot using a standardized and repeatable procedure.

For the axial impact case, the updated THUMS AM50 model closely aligned with PMHS experimental data.

Compared to the baseline model, the updated version demonstrated a slightly stiffer response before reaching peak force (6200 N vs. 6000 N for the updated and baseline models, respectively), followed by a softer post-peak response. Overall, the force-displacement response of the updated model remained within the PMHS biofidelity corridors.

In the dorsiflexion loading scenario, the updated model exhibited improved agreement with PMHS data, whereas the baseline model displayed a stiffer response. For a 40° calcaneus rotation, the ankle moment was 25 Nm in the updated model, compared to 50 Nm in the baseline model. This result confirms that the modifications applied to the ankle ligaments and cartilage improved the biofidelity of the model. Furthermore, analysis of ligament cross-sectional forces revealed that the updated model achieved more balanced load distribution among the ligaments. In contrast, the baseline model exhibited force concentration in the posterior tibiotalar ligament, which reached a peak force of 2400 N. This was substantially higher than experimental findings reported by [11] and [14–15], where failure forces for ankle ligaments tended to range from 130 to 600 N. If the internal load distribution were dominated by a single ligament (as suggested with the baseline model), then one would expect that ligament to be the most commonly injured ligament in the field and in PMHS tests. Instead, the actual ankle injury patterns in field data and PMHS studies are much more varied [16]. The updated model, in contrast, exhibited a max ligament force of ~350 N, which was within the range that could potentially be injurious, but without a single ligament dominating the response.

In the inversion loading case, the updated model demonstrated a slightly stiffer response compared to the baseline model. For a 30° calcaneus rotation, the ankle moment reached 70 Nm in the updated model compared to 50 Nm in the baseline model, while still aligning with PMHS response trends.

For eversion loading, the updated model initially exhibited a slightly stiffer response compared to PMHS results; however, the overall trends were well-aligned. At 40° of calcaneus rotation, the ankle moment was 182 Nm for the updated model, compared to 280 Nm in the baseline model. The baseline model, in contrast, showed a much stiffer response when compared to both the updated model and PMHS data. This increased stiffness may be attributed to differences in the initial foot posture between the PMHS test and the simulation.

Analysis of ligament cross-sectional forces in inversion and eversion cases further confirmed greater load distribution in the updated model. By contrast, the baseline model exhibited dominance of a single ligament bearing most of the load. The adjustment of insertion points and updated material properties facilitated greater elongation (average of ~8 mm increase), enabling a better redistribution of forces across multiple ligaments. This increased load distribution enhances the overall biofidelity of the model, particularly under eversion loading conditions.

Overall, this study represents a substantial advancement in the ongoing research and refinement of THUMS AM50 aimed at improving ankle injury prediction and prevention in MVCs. The modifications applied to the THUMS AM50 model have enhanced the anatomical accuracy and biomechanical fidelity of the ankle joint, leading to improved validation performance across multiple loading scenarios. The validation cases considered in this study replicate key loading modes associated with ankle injuries in MVCs. The results demonstrate that cartilage and ligament enhancements improved force transmission between articulating bones and load distribution between ligaments. Additionally, the inclusion of a shoe model enhances the HBM crash simulations by more accurately representing shod-foot loading conditions commonly encountered in real-world crash events. These advancements collectively can help improve the predictive capabilities of HBMs for lower extremity injuries, providing a more reliable platform for researching injury risk and future automotive safety systems. Further refinement of the model, including additional validation cases and parameter optimization, will continue to enhance its utility in injury biomechanics research.

Limitations

Previous efforts to integrate a shoe with the THUMS AF05 model benefitted from having small female validation data available with tests performed with and without shoes [5]. The THUMS AM50 model with the integrated shoe was not validated in this study due to the limited availability of PMHS data involving mid-sized male lower extremities tested with low-ankle footwear. Although several studies have tested lower extremities with high-ankle boots [17-19], the different style was deemed not comparable for biomechanical responses related to loading and injury mechanisms in automotive tests and field data generally. Thus, additional PMHS data may be needed to validate the performance of the THUMS AM50 with relevant shoes. Further, the existing shoe model represents a Mil-Spec shoe that, while commonly used with anthropomorphic test devices (ATDs), may not be representative of everyday shoes typically worn by the population. Further investigation could include studying the influence of different designs or stiffnesses of shoes on ankle loading to determine if developing different shoe models is warranted.

V. CONCLUSION

Ankle fractures are among the most frequently observed AIS2+ injuries in motor vehicle collisions (MVCs), often resulting from complex, multi-modal loading conditions. This study aimed to enhance the anatomical accuracy, biomechanical fidelity, and predictive capability of the foot and ankle model in the THUMS v.6.1 50th percentile male human body model (HBM). Key refinements included improvements to ligament morphology and insertion points, as well as the addition of cartilage at the articulating surfaces of four primary ankle joints to improve load distribution and joint response. The updated model was evaluated for the biofidelity validation through four loading scenarios—axial compression, dorsiflexion, inversion, and eversion—replicating PMHS experiments conducted under unshod conditions. Subsequently, a shoe model was integrated using a fitting approach to achieve a secure and realistic fit. With these refinements and enhancements, the updated THUMS AM50 foot-ankle model provides a more accurate foundation for investigating ankle injury mechanisms in simulated automobile crashes, ultimately contributing to the advancement of occupant safety research.

VI. ACKNOWLEDGEMENTS

This work was funded by the Toyota Collaborative Safety Research Center CSRC). The authors also acknowledge Research Computing at The University of Virginia for providing access to computational resources and technical support that have contributed to the results reported within this publication.

VII. REFERENCES

[1] Forman, J., Poplin, G. S., *et al.* (2019) Automobile injury trends in the contemporary fleet: Belted occupants in frontal collisions. Traffic injury prevention, **20**(6): pp.607–12.
[2] Craig, M. J., Liu, C., Zhang, F., Enriquez, J. (2024) Sex-based differences in odds of motor vehicle crash injury outcomes. Accident Analysis & Prevention, 195, 107100.
[3] van den Bekerom MPJ, Raven EEJ. The distal fascicle of the anterior inferior tibiofibular ligament as a cause of tibiotalar impingement syndrome: a current concepts review. Knee Surg Sports Traumatol Arthrosc. 2007 Apr;15(4):465-71. doi: 10.1007/s00167-006-0275-7. Epub 2007 Jan 20. PMID: 17237964; PMCID: PMC1915597.
[4] Golanó, P., Vega, J., de Leeuw, P. A., Malagelada, F., Manzanares, M.C., Götzens, V., van Dijk, C.N. (2010) Anatomy of the ankle ligaments: a pictorial essay. Knee Surg Sports Traumatol Arthrosc. **18**(5):pp. 557–69.
[5] Iyer, R., Caudillo-Huerta, A., Gepner, B., Hallman, J., Panzer, M., Forman, J., (2024) Refinement and Biofidelity Evaluation of the THUMS Small Female Ankle. IRCOBI Conference Proceedings 2024, Sweden.
[6] Mukherjee, S., Zeng, W., Roberts, C., Caudillo, A., Forman, J., Panzer, M. (2022) Validation of small female foot and ankle finite element model under shod automotive loading environment. IRCOBI Conference Proceedings 2022, Porto, Portugal.
[7] Ushinosuke, Kaneko, "Japanese Human Anatomy (Revised 19th Edition), Volume 1", ISBN 978-4-525-10089-3
[8] Ushinosuke Kaneko, "Japanese Human Anatomy (Revised 19th Edition), Volume 2", ISBN 978-4-525-10099-0
[9] Frank H.Netter, "Netter's Atlas of Anatomy (5th Edition)“, Frank H.Netter, ISBN 978-4-524-26969-3
[10] Rene Cailliet, "Functional Anatomy of the Musculoskeletal System", ISBN 978-4-263-21111-1
[11] Funk, J.R., Tourret, L.J., George, S.E., Crandall, J.R., (2000) The Role of Axial Loading in Malleolar Fractures. SAE World Congress.
[12] Rudd, R., Crandall, J.R., Millington, S., Hurwitz, S., Joglund, N., (2004) Injury Tolerance and Response of the Ankle Joint in Dynamic Dorsiflexion. 48th Stapp Car Crash Conference, 2004, Nashville, Tennessee.
[13] Funk, J.R., Srinivasan, SCM, *et al.* (2002) The Effects of Axial Preload and Dorsiflexion on the Tolerance of the Ankle/Subtalar Joint to Dynamic Inversion and Eversion. 46th Stapp Car Crash Conference, 2002, Ponte Vedra Beach, Florida.
[14] Nie, B., Panzer, M., *et al.* (2017) Determination of the in situ mechanical behavior of ankle ligaments, Journal of the Mechanical Behavior of Biomedical Materials, **65:** pp.502– 512.
[15] Funk, J. R., Hall, G. W., Crandall, J. R., Pilkey, W. D,. (2000) Linear and quasi-linear viscoelastic characterization of ankle ligaments. J. Biomech. Eng., **122**(1): pp.15–22.
[16] Funk, J. R. (2011) Ankle injury mechanisms: lessons learned from cadaveric studies. Clinical anatomy, **24**(3): pp.350– 361.

[17] de Lange, J., Quenneville, C.E. (2020). Investigation of the Biofidelity of the MIL-Lx Foot. IRCOBI Conference Proceedings. (No. IRC-20-77)
[18] Quenneville CE, Dunning CE. Evaluation of the biofidelity of the HIII and MIL-Lx lower leg surrogates under axial impact loading. Traffic Inj Prev. 2012;13(1):81-5. doi: 10.1080/15389588.2011.623251. PMID: 22239148.
[19] Bir C, Barbir A, Dosquet F, Wilhelm M, van der Horst M, Wolfe G. Validation of lower limb surrogates as injury assessment tools in floor impacts due to anti-vehicular land mines. Mil Med. 2008 Dec;173(12):1180-4. doi: 10.7205/milmed.173.12.1180. PMID: 19149335.